

## Fast relaxation of a hexagonal Poiseuille shear-induced near-surface phase in a threadlike micellar solution

W. A. Hamilton,<sup>1</sup> P. D. Butler,<sup>2</sup> L. J. Magid,<sup>3</sup> Z. Han,<sup>3</sup> and T. M. Slaweki<sup>2</sup>

<sup>1</sup>*Solid State Division, Oak Ridge National Laboratory, Oak Ridge, Tennessee 37831-6393*

<sup>2</sup>*National Institute of Standards and Technology, Gaithersburg, Maryland 20899*

<sup>3</sup>*Department of Chemistry, University of Tennessee, Knoxville, Tennessee 37996*

(Received 5 January 1999; revised manuscript received 14 May 1999)

The dynamics of near-surface conformations in complex fluids under flow should dramatically affect their rheological properties. We have made the first measurements resolving the decay kinetics of a hexagonal phase induced in a threadlike polyionic micellar system under Poiseuille shear near a quartz surface. Upon cessation of shearing flow, this minimum interference crystalline phase formed within  $\sim 20 \mu\text{m}$  of the surface “melts” to a metastable two-dimensional liquid of aligned micelles in  $\sim 0.7$  s. This is some three orders of magnitude shorter than the time required for bulk (Couette) shear-aligned micelles in this system to reach a fully entangled state. [S1063-651X(99)50808-8]

PACS number(s): 82.70.Dd, 61.12.Ex, 61.25.Hq, 83.50.By

In aqueous solution some surfactants aggregate into threadlike micelles, highly extended structures a few nm in radius but with contour lengths of order micron, which entangle giving rise to complex fluid properties similar to those of long chain polymer solutions. However, as self-assembled structures, these micelles continually break and recombine in an interplay strongly affected by the micellar charge arrangement, since the binding and species of counterion and any supporting electrolyte alters the electrostatic screening of amphiphile headgroups and the micellar stiffness. These systems display a rich variety of microscopic orderings and mesoscopic phase responses to flow. The earliest small-angle neutron scattering (SANS) studies used hydrodynamic alignment along flowlines to determine individual micellar structures [1,2]. Later investigations noted bulk shear-induced micellar elongation and consequent shear thickening [3], so-called “shear band” textures [5], and work by our group noted the Poiseuille shear-induced crystalline ordering under flow near interfaces [4], whose dynamics are the subject of this Rapid Communication. More recently, small-angle light scattering investigations have revealed shear-induced phase separations [6] and flow-aligned mesoscopic string phases of concentration above the bulk average [7].

In the work presented here we investigate the kinetics of a near-surface hexagonal phase we have observed in the threadlike micellar mixed counterion system consisting of the surfactants cetyltrimethylammonium 3,5 dichlorobenzoate and CTABromide in 70:30 ratio at 20 mM concentration in aqueous solution ( $\sim 1$  wt%). The rheology of this system is relatively complex. The micelles have a significant linear charge density making them relatively stiff and the entangled micellar network in solution is not only viscous, but strongly viscoelastic. Under flow the solution thins dramatically as the initially entangled micelles align [12]. Our group has developed near-surface small-angle scattering (NS-SANS) techniques to measure complex fluid states under Poiseuille shearing flow in close proximity to a surface [8]. In our sample cell the solution is pumped through a shallow (depth  $d=1$  mm) trough beneath a slab of polished quartz [9]. A neutron beam incident through the quartz slab at grazing angle to the quartz-solution interface undergoes

partial specular reflection at the interface and partial transmission into the solution. The macroscopic cross section of this solution is  $0.9 \text{ cm}^{-1}$  and, at the transmitted beam’s small angle ( $\sim 0.2^\circ$ ) to the interface, allows penetration to only a few tens of  $\mu\text{m}$  in depth beyond the quartz surface; this allows us to use scattering of the transmitted beam to probe the fluid in the shearing flow near the interface. At zero flow the off-specular signal is very weak scattering of the transmitted beam by the entangled micelles. However, under flow the specular reflection signal is surrounded by a clear small-angle hexagonal diffraction pattern from transmitted beam scattering, showing that the initially entangled micelles not only align along the flow direction but also “crystallize” into a hexagonal array strongly oriented with respect to the surface along the whole near-surface flow path [Fig. 1(a)]. Moreover, this is a distinct mesoscopic flow phase, which apparently, for its stability, depends on the proximity of the interface. Using the crystal parameters derived from the diffraction patterns it can be shown that the scattering observed for this system, over Couette bulk shear gaps (0.5 mm) in the same shear regime, is inconsistent with any significant presence of the hexagonal phase in the bulk shear field (either fully oriented with respect to the shear flow field or rotationally “powder” averaged about the flow direction). The data rather indicate a two-dimensional (2D) liquid ordering of the aligned micelles across the plane perpendicular to the flow direction [10].

As the schematic of the micellar flow pattern of Fig. 1(a) suggests, we can expect the existence of this phase to have strong rheological consequences. Obviously, micelles in the crystal lattice planes parallel to the interface [the (01), hexagonally indexed] can move easily past each other as a whole in the near-surface region, with minimal interference of the micelles with each other and the interface. In our measurements, planes parallel to the quartz-solution interface are separated by 39 nm (8.5 times their 4.6 nm micellar diameter). For our near-surface Poiseuille shear rates,  $\dot{\gamma} \sim 250 \text{ s}^{-1}$ , succeeding layers have relative velocities of  $\sim 10\,000 \text{ nm/s}$ . In contrast, for a liquid ordering, a micelle’s nearest neighbors will be at different depths and will *all* be in

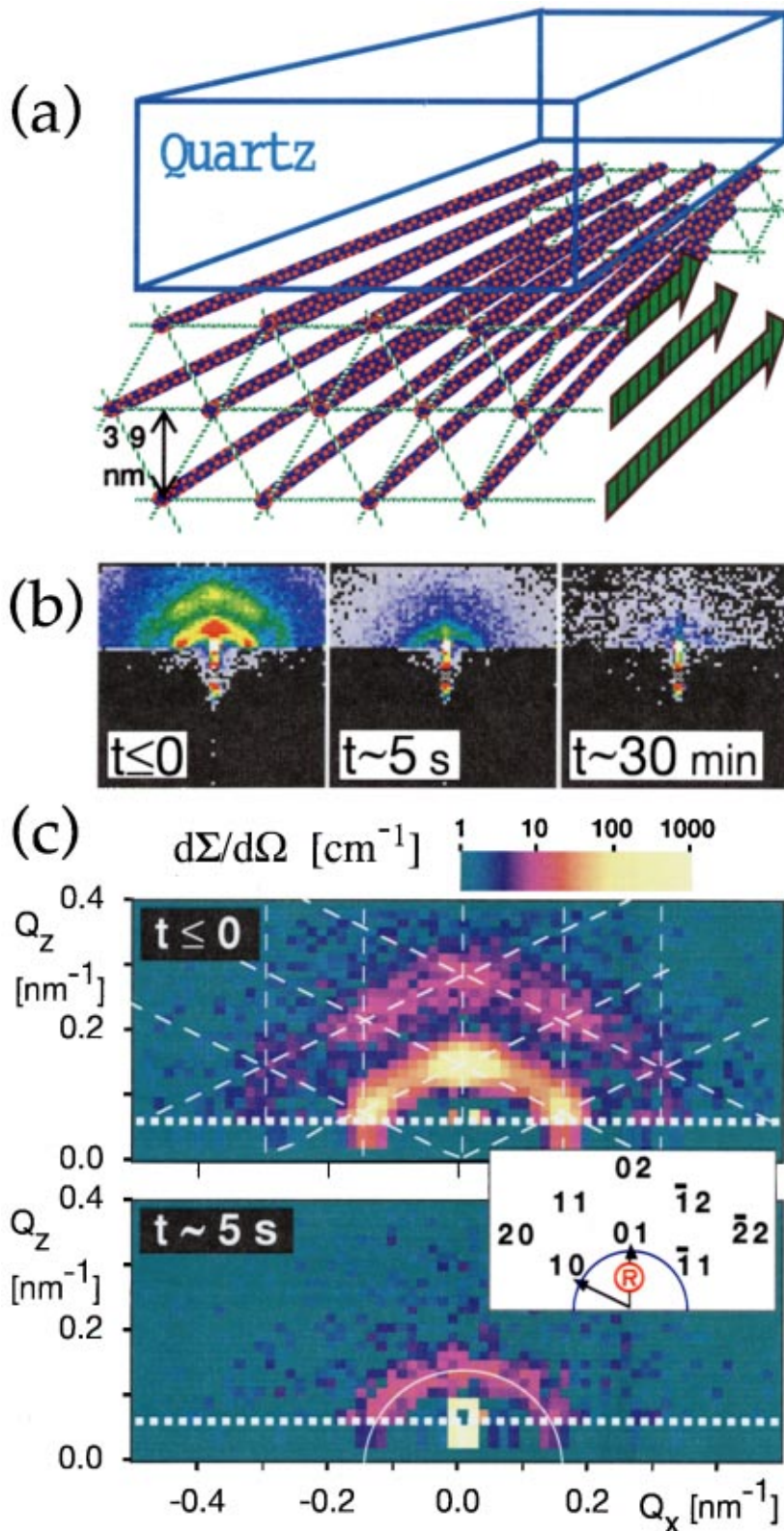


FIG. 1. (Color) (a) Schematic of hexagonal near-surface Poiseuille shear-induced micellar ordering. The arrows show the velocity of (01) planes in laminar flow. The incident beam for NS-SANS measurements is along the flow direction glancingly incident upon quartz-solution interface. (b) The raw SANS data:  $t \leq 0$  and  $t \sim 5$  s (summed 0.5 binning time slices), and  $t \sim 30$  min. (c) The refraction corrected scattering patterns for the fully aligned  $t \leq 0$  and partially relaxed  $t \sim 5$  s data. The overlays indicate the hexagonal lattice and the ring ( $\curvearrowright$ ) for the  $t \sim 5$  s relaxed state. The neutron wavelength was  $0.5 \text{ nm} \pm 10\%$  and the angle of incidence to the quartz-solution interface  $\theta = 0.280^\circ$ , corresponding to a specular reflectivity vector transfer  $Q_R = 0.124 \text{ nm}^{-1}$ . This is above the critical wave vector for total external reflection at the interface ( $Q_c = 0.10 \text{ nm}^{-1}$ ,  $\theta_c = 0.23^\circ$ ) and the reflection coefficient at the interface is 20%, so the probe beam transmission into the solution is 80% refracted to an angle of  $0.16^\circ$ . To exit the cell a neutron must be scattered back toward the quartz-solution interface, i.e., at  $> 0.32^\circ$ . This corresponds to a limiting horizon for observable *in-solution* scattering  $Q_z \geq (Q_R^2 - Q_c^2)^{1/2} = 0.07 \text{ nm}^{-1}$ , indicated by dotted lines. The inset shows the indexing of the diffraction spots, with the apparent relative position of the specularly reflected beam designated  $R$ . The residual difference after subtraction of the strong specular signal is not statistically significant.

relative motion of this order. It seems likely that the dynamics of this near-surface phase should strongly affect to the solution's microrheology, with properties depending on micellar entanglement and interference such as the liquid's drag and stick-slip response to shear and flow changes governed by its crystallization and relaxation times. Couette measurements on bulk shear ordering show alignment and decay times for this system of order 20–40 min [11]. Our initial

measurements using the 30 m SANS instrument at the Oak Ridge National Laboratory could only determine that this near-surface phase's decay was at least an order of magnitude faster.

In order to better track this rapid response to shear flow changes, we employed the National Institute of Standards and Technology SANS instrument NG3 in "the time slicing" mode: triggered acquisition of SANS data to histo-



gramming memory in a series of constant width time bins. Synchronizing the trigger with the cycled operation of our Poiseuille shear cell allows the accumulation of statistically significant scattering measurements on much shorter time scales than is possible for individual runs. In order to fully resolve the relaxation process reported here, time binning was done in two separate runs using available bin intervals 0.5 s and 0.1 s over the instrument's 16 bin range. The initial alignment of the micellar system during each cycle was done over 20 s at an average cell flow speed  $\bar{v}$  of 10 mm/s. This was the lowest flow velocity giving a fully saturated hexagonal ordering signal in steady-state measurements and corresponds to a shear rate in the first few  $10^3$ 's of  $\mu\text{m}$  from the quartz surface of  $\dot{\gamma} \sim 200\text{--}450\text{ s}^{-1}$  [12]. Data acquisition was triggered 1.0 s and 0.5 s, respectively, before the signal to stop the shear cell pump so that initial data bins allowed verification of full hexagonal ordering of the system before the cessation of shear. Neutron scattering patterns for the 8 s and 1.6 s spanned by the two time binning schemes were accumulated over approximately 1000 cycles in each case for elapsed times of 8 h with a 30% duty cycle for the 0.5 s binning and 6.5 h at 7% for the 0.1 s binning (an extra 2 s relaxation was added to the end of these cycles).

Time-sliced measurements allow us to identify two stages in the Poiseuille shear relaxation in this system [Fig. 1(b)]. For  $t \leq 0$  [ $-1 < t < 0$  s] the diffraction pattern surrounding the specularly reflected beam indicates full shear ordering of the micelles in the near-surface region along the flow direction in a hexagonal array strongly oriented with respect to the quartz-solution interface. Upon cessation of shear at  $t = 0$ , although the micelles remain aligned, the off-specular scattering falls within seconds by about an order of magnitude from the  $t \leq 0$  first order diffraction peak values, and a correspondingly rapid loss of orientational order results in the ring of scattering visible in  $t \sim 5$  s data [3.5  $< t < 6.5$  s]. Only over a longer time period ( $t \sim 30$  min), consistent with the bulk decay time from an aligned to a fully entangled micellar state in bulk scattering measurements, does the observed off-specular ring scattering fall (by about a factor of 2) to a weaker background level of scattering from fully entangled micelles in the static solution. In Fig. 1(c) the SANS scattering patterns have been corrected for refractive distortion and scattering volume effects to give *in-solution* differential scattering cross-section  $d\Sigma/d\Omega$  for  $t \leq 0$  and  $t \sim 5$  s data. Subtraction of the  $t \sim 30$  min fully relaxed "background" signal eliminates the stronger specular reflection signal, parasitic slit scattering in the reflection plane and the bulk scattering contribution [13].

The strength of the ring of scattering in the  $t \sim 5$  s data relative to that of the fully relaxed  $t \sim 30$  min signal shows that the micelles initially remain aligned along the former flow direction. Two possibilities are suggested by the ring itself. Either (i) The hexagonal crystalline ordering, the minimum state of electrostatic potential energy, is initially maintained locally, but has lost the strong orientation provided by the hydrodynamic field. In this case the ring is simply the rotationally averaged powder pattern of the first order hexagonal diffraction peaks or (ii) The ring represents the first strong ring of nearest neighbor scattering from a two-dimensional liquid of aligned micelles. In this latter case we

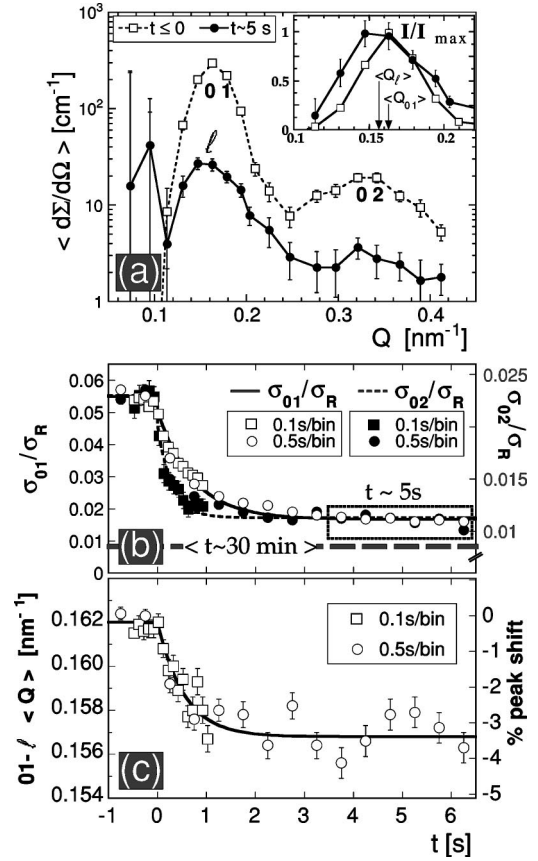


FIG. 2. (a) Differential cross section averaged within  $\pm 10^\circ$  of the  $Q_z$  axis for the  $t \leq 0$  s and  $t \sim 5$  s data. This encompasses the positions of the 01 and 02 diffraction spots for the  $t \leq 0$  s data, while the scattering ring position for the  $t \sim 5$  s data is indicated by the script  $\ell$ . Inset: 01 and  $\ell$  peaks scaled to their maxima showing the shift in the scattering position. (b) The time evolution of the integrated 01 scattering peak cross section,  $\sigma_{01}$ , here and Fig. 2(c); left hand scale, open symbols; and for the 02 peak  $\sigma_{02}$ , right hand scale, full symbols. Normalization is to the total specular reflection cross section,  $\sigma_R$ . The background scattering level for the 01/ $\ell$  region at  $t \sim 30$  min is indicated by the dashed horizontal line. (c) The time evolution of the mean scattering peak position in the 01/ $\ell$  region.

can expect a shift between the  $Q$  of the first order crystalline diffraction peaks and the ring. The scattering intensity  $I(Q)$  for a two-dimensional liquid is given by the integral over the pair correlation function multiplied by  $J_0(Qr)$ . Taking the derivative of  $I(Q)$  with respect to  $Q$  and assuming that the pair correlation function has a well defined peak at the nearest neighbor distance,  $r_{nn}$ , the first observable maximum in  $(Q \neq 0)$  in the liquid scattering corresponds to the third zero in  $J_1(Qr_{nn})$ , which occurs for  $Q = 7.016/r_{nn}$  [14]. The first order diffraction peaks for a hexagonal lattice occur at  $Q = 2\pi/(\sqrt{3}r_{nn}/2) = 7.255/r_{nn}$ . Simply assuming constant density and that the nearest neighbor distances are the same for both phases, a liquid ring peak may be expected to occur at a  $Q$  value 3.3% less than observed for first order diffraction spots. Figure 2(a) shows a sector cut of  $d\Sigma/d\Omega$ , averaged within  $\pm 10^\circ$  of the  $Q_z$  axis, as a function of scattering vector for the  $t \leq 0$  and  $t \sim 5$  s data. Comparison of mean scattering intensity position of the 01 first order diffraction and ring ( $\ell$ ) scattering peak region ( $0.11 \leq Q_z$

$\leq 0.21 \text{ nm}^{-1}$ ,  $|Q_x| \leq 0.06 \text{ nm}^{-1}$ ) for the 0.5 s binning runs shows a relative shift [15] from  $\langle Q_{01} \rangle = 0.1623 \pm 0.0002 \text{ nm}^{-1}$  to  $\langle Q_{\rho} \rangle = 0.1568 \pm 0.0004 \text{ nm}^{-1}$  as the system relaxes, a decrease of  $3.4 \pm 0.3\%$ , consistent with the conclusion that the hexagonal lattice has indeed undergone rapid two-dimensional melting upon the cessation of shear [16].

The time evolution of the relaxation was tracked by summing the scattering over the region of crystalline diffraction peaks for each time bin. Figure 2(b) shows the integrated cross section,  $\sigma_{01}$ , of the strong 01 diffraction spot region for the 0.5 s and 0.1 s binning runs (full symbols/left hand scale), normalized against the signal of the specularly reflected beam  $\sigma_R$ , which was constant within experimental error. A decay time of  $0.7 \pm 0.2 \text{ s}$  for this peak was obtained by fitting the combined data (allowing for binning integration). After the initial rapid decay the scattering in this region falls only slowly to the fully relaxed state background level for ( $t \sim 30 \text{ min}$ ) shown as a horizontal line. The other observable first order diffraction spots (10 and  $\bar{1}1$ ) decay at the same rate as the 01. As we would expect the mean  $Q$  position of the 01 scattering shifts with the same characteristic time as the intensity decays [Fig. 2(c)]. However, the decay of the higher order diffraction peaks is rather faster than for the first order. From consideration of the Debye-Waller Bragg scattering intensity reduction factor  $\exp\{-Q^2\langle[\Delta r(t)]^2\rangle/2\}$ , where  $\langle[\Delta r(t)]^2\rangle$  is the mean square displacement from the exact lattice position at time  $t$ , we expect that the decay rate should go roughly as  $Q^2$  of the Bragg peak [17]. The decay time for the second order 02 peak cross section,  $\sigma_{02}$ , is indeed about a factor of 4 smaller at  $\sim 0.1-0.2 \text{ s}$  [full symbols/right hand scale in Fig. 2(b)]. Unfortunately, resolution of a decay time of this order at the required duty cycle

( $< 2\%$ ) would be prohibitively time consuming and would require improved control of the stopping time of our shear cell pump ( $\sim 0.05 \text{ s}$ ).

In conclusion, the relaxation of the near-surface oriented crystalline phase measured here is about three orders of magnitude faster than the full relaxation of the micelles to an entangled state seen in the bulk shear measurements. The high-intensity NS-SANS technique, coupled with time slicing, shows that this hexagonal phase melts to a much longer lived 2D liquid alignment consistent with those bulk measurements and clearly demonstrates the near-surface Poiseuille shear-induced nature of the hexagonal state. Although hydrodynamic alignment of the micelles persists, it is not sufficient to maintain even local crystalline ordering. Finally, we note that the rheological response implications for this and similar systems of technological importance may be quite dramatic. One might expect that the crystalline phase change at the surface effectively creates a very low viscosity (minimum interference) mesoscopic "slip" layer capable of easily supporting very high shear gradients and conforming relatively rapidly to flow changes, therefore, effectively lubricating the movement past the surface of domains of less organized micellar alignments at greater distances from the interface.

We would like to thank M. Yethiraj, J.L. Robertson, and J.B. Hayter of ORNL, B. Hammouda, J. Reardon, and C. Glinka of NIST, Oak Ridge National Laboratory, managed by Lockheed Martin Energy Research Corporation under Contract No. DE-AC05-96OR22464 with the U.S. Department of Energy, and the National Science Foundation (L.J. Magid, Grant No. CHE-9729433). The NIST NG3 SANS instrument is supported by the NSF under Agreement No. DMR9423101. The identification of equipment or materials does not imply recommendation by NIST.

- 
- [1] J.B. Hayter and J. Penfold, *J. Phys. Chem.* **88**, 4589 (1984).  
 [2] Ch. Thurn, J. Kalus, and H. Hoffmann, *J. Chem. Phys.* **80**, 3440 (1984).  
 [3] V.K. Jindal *et al.*, *J. Phys. Chem.* **94**, 3129 (1990).  
 [4] W.A. Hamilton *et al.*, *Phys. Rev. Lett.* **72**, 2219 (1994); **74**, 335 (1995).  
 [5] D.C. Roux *et al.*, *Macromolecules* **28**, 1681 (1995).  
 [6] T. Kume and T. Hashimoto, in *Flow Induced Structure in Polymers* (American Chemical Society, Washington, D.C., 1995), Vol. 597, p. 35.  
 [7] I.A. Kadoma and J. van Egmond, *Phys. Rev. Lett.* **80**, 5679 (1998).  
 [8] W.A. Hamilton *et al.*, *Physica B* **221**, 309 (1996).  
 [9] S.M. Baker *et al.*, *Rev. Sci. Instrum.* **65**, 412 (1994).  
 [10] P.D. Butler *et al.*, *Faraday Discuss.* **104**, 65 (1996); **104**, 88 (1996);  
 [11] P.D. Butler *et al.*, *J. Phys. Chem.* **100**, 442 (1996).  
 [12] Unpublished Couette viscometer measurements by T.L. Smith and L.J. Magid indicate that 20 mM 70:30 CTA35CIBz/Br is a "power law" fluid with a coefficient  $n$  of 0.05 ( $n = 1$  for Newtonian fluids). Our estimates of near-surface shear rates vs flow speed for the Poiseuille cell are based on the power law fluid treatment in R.J. Hunter, *Foundations of Colloid Science* (Clarendon, Oxford, 1989), Vol. II, Chap. 11. Assuming this fluid behavior, the maximum shear rate at the interface is  $\dot{\gamma}_{max} = (4 + 2/n)\bar{v}/d$ .  
 [13] For details of reflection geometry cell SANS data correction see Refs. [4] and [8].  
 [14] The derivation is directly analogous to that for a 3D liquid system; see, for instance, J.M. Schultz, *Diffraction for Materials Scientists* (Prentice-Hall, Englewood Cliffs, NJ, 1982), Ch. 2, p. 43; M. Yethiraj *et al.*, *Phys. Rev. Lett.* **78**, 4849 (1997) applied this 2D argument to magnetic flux lattices in superconductors.  
 [15] Errors in the mean  $Q$  of the peak distribution are relative to the SANS calibration used for our simultaneously collected measurements at constant geometry. The absolute accuracy of the  $Q$  determination, the error applicable when comparing independent SANS sample measurements, would be an order of magnitude larger.  
 [16] Note that if we instead postulate that the metastable  $t \sim 5$  s state of the system is polycrystalline, we must also infer (and explain) a  $\sim 7\%$  decrease in micelle concentration simultaneous with the decay.  
 [17] If we define an effective 2D translational diffusion coefficient, such that  $\langle[\Delta r(t)]^2\rangle = \langle[\Delta r(0)]^2\rangle + Dt$ , the 0.7 s decay we observe for the 01 peak at  $Q = 0.16 \text{ nm}^{-1}$  corresponds to  $D = 110 \text{ nm}^2/\text{s}$ .